Received 31 August 2023; revised 23 October 2023 and 26 October 2023; accepted 26 October 2023. Date of publication 28 November 2023; date of current version 21 December 2023. The review of this article was arranged by Editor Paolo Bonato.

Digital Object Identifier 10.1109/OJEMB.2023.3336181

Targeted Sensitization of Glioblastoma Multiforme Using AAAPT Technology

MEGAN MENDIETA [1] (Student Member, IEEE), NAZE G. AVCI [1], RAGHU PANDURANGI [2], YASEMIN M. AKAY [1] (Senior Member, IEEE), AND METIN AKAY [1] (Life Fellow, IEEE)

[1]University of Houston, Houston, TX 77204 USA
[2]Sci-Engi-Medco Solutions Inc., Saint Charles, MO 63303 USA

CORRESPONDING AUTHOR: METIN AKAY (e-mail: makay@uh.edu)

The work of Raghu Pandurangi was supported by NIH SBIR under Grant R43CA214223 to carry out the synthesis and characterization of AMPs. The work of Metin Akay was supported by The University of Houston for the 3D drug screening studies, and genomic and proteomic analysis.

ABSTRACT Glioblastoma Multiforme (GBM) is the most malignant type of all brain tumors. Current GBM treatment options include surgery, followed by radiation and chemotherapy. However, GBM can become resistant to therapy, resulting in tumor recurrence. GBM cells develop resistance to treatments by either downregulating cell death pathways (CD95) or upregulating cell survival pathways (NF-κB (p65)). Healthy tissues can be affected by the increased therapeutic dose. Therefore, it is important to develop a method that can only target GBM tumor cells, thereby reducing the non-specific uptake which will reduce the side effects. Here we demonstrate an application of novel priori activation of apoptosis pathways of tumor technology (AAAPT), which has been used to demonstrate the effect of targeted tumor sensitizers to make chemotherapy work at lower doses in breast, lung and prostate cancers. Treatment of GBM spheroids with AAAPT in 3D PEGDA microwells, showed an increase in cell death, an upregulation of cell death pathways, and a downregulation of cell survival pathways, in comparison to Temozolomide (TMZ), an oral alkylating agent, which is a commonly used chemotherapy in the treatment of GBM. The dose of AAAPT sensitizers may provide a promising method to increase treatment efficacy and reduce off-target toxicity, as an alternative to existing methods which cause significant off-target damage.

INDEX TERMS Spheroids, glioblastoma, co-treatment, tumor microenvironment, PEGDA.

IMPACT STATEMENT Microwell-generated GBM spheroids are sensitized by AAAPT drugs using targeted, cleavable linkages to reduce off-target toxicity.

I. INTRODUCTION

Glioblastoma Multiforme (GBM) is the most aggressive astrocytic tumor accounting for 47.7% of all Central Nervous System (CNS) tumors [1] and for almost 80% of all malignant primary brain tumors [2], [3]. Standard of care includes surgical resection, followed by a combination of radiation and chemotherapy. Despite these treatments, disease recurrence is frequent, where only 3% to 5% of GBM patients live past three years after diagnosis[4,5]. Temozolomide (TMZ), a DNA alkylating agent, is the commonly prescribed chemotherapy drug, however in the tumors expressing the direct repair protein O6-methylguanine-DNA methyltransferase (MGMT), TMZ resistance is commonly observed [6], [7], [8]. Tumors possess the ability to reduce expression of cell death pathways and increase expression of cell survival pathways, reducing treatment effectiveness [9], [10], [11]. Due to the low survival rate in considering a standard chemotherapy treatment, there is a critical need to develop new regimens, discover novel potential targets, and establish new assets for protecting the efficacy of GBM treatment in each patient.

Previous studies conducted by our lab utilize a 3D PEGDA-based hydrogel microwell platform, in which spheroids can aggregate up to 400 μm in diameter, to provide a novel in vitro platform for longitudinal cancer studies with support for

selective suppression of tumor growth and angiogenesis [12]. Screening of potential treatments via in vitro culture of 3D tumors, such as spheroids, has shown to better recapitulate tumor attributes, than 2D culture, and are cost-effective [13], [14], [15], [16], [17]. The platform demonstrated that the addition of the synergistic drug, BAY11-7082, an inhibitor of κB kinase (IKK), suppressed GBM cell survival pathway expression by inhibiting DNA repair and increased apoptotic activity [18]. Furthermore, co-culture studies conducted previously with the microwell system demonstrated the ability of the platform to help define microenvironmental effects on treatment [19].

A priori activation of apoptosis pathways of tumor technology (AAAPT) was developed to attack modulate dysregulated cell death pathways which are the basis of mechanism of cell desensitization [20], [21]. AMP-001-003, were synthesized to be cleavable by the tumor specific secretion of Cathepsin B [21], [22], [23]. Triple negative breast cancer cells cultured in 3D were treated with AMP-001, resulting in increased apoptosis activity, suppression of cell survival pathways, and triggering of cell death pathways [20]. Cardiac tissue treated in parallel saw little cytotoxic effect, demonstrating the drug's specificity and reduction of off-target effects, commonly experienced in standard chemotherapy regimens.

The BCL-2 family proteins contribute to the resistance of glioma cells to anticancer therapy by modulating the apoptotic cascade, where BCL-2 is an inhibitor of apoptosis and BAX promotes cell death [24], [25]. NF-κB also serves to upregulate antiapoptotic genes, while CD95 recruits proapoptotic factors [26], [27], [28], [29], [30]. In this study, we hypothesize that treatment of GBM with novel tumor targeted sensitizer, AMP-001, may increase the apoptotic activity and act as a more specific treatment for GBM as opposed to Temozolomide, which is an oral alkylating agent used for the first-line therapy of GBM. Investigating these expression patterns in relation to AMP-001 would verify the pathways causing GBM to decrease in cell viability and could establish more targets for future therapies. Here, we investigate a high throughput screening of GBM cells via real-time PCR (RT-qPCR) and Western Blot to investigate gene and protein expressions and subsequently, the mechanisms for sensitization of resilient GBM cancer cells.

II. MATERIALS AND METHODS

A. CELL LINES AND CELL CULTURE

Glioblastoma cell line LN229 was purchased from the American Tissue Culture Collection (ATCC) (Manassas, VA). LN229 cells were cultured in cell culture plate up to passage 16, using Dulbecco's modified Eagle's medium (DMEM) (Gibco, USA) supplemented with 10% FBS (HyClone, USA), and 1% of 100 U/mL penicillin and 100 g/mL streptomycin (Gibco, USA). All cells were stored in a cell culture incubator at 5% CO2, 37 °C.

B. PEGDA MICROWELL FABRICATION AND 3D SPHEROID CULTURE

Fabrication of PEGDA Microwells was conducted as described previously [12]. 25 × 25 mm cover glass slides were treated with 3-(Trimethoxysilyl) propyl methacrylate 98% (TMSPMA) (Life Technologies, New York, NY, USA). The slides were first layered with a 20 μL of 40% (w/w) PEGDA (MW 700) (Life Technologies, New York, NY, USA), 0.2% (w/v) photoinitiator (PI) 2-hydroxy-2-methyl propiophenone, Phosphate Buffered Saline (PBS) (Life Technologies, New York, NY, USA) solution. They were then exposed to Lumen Dynamics the OmniCure Series 2000 (Lumen Dynamics Group Inc, Mississauga, ON, Canada) for 35 seconds at a working distance of 6 inches. Next, 250 μL of PEGDA solution was added to the slide and cured in UV light for 36 seconds with a photomask (CADart, Bandon, OR, USA) with 400 μm diameter dots in a grid pattern, on top. Prepared slides were washed and incubated overnight in 6-well plates containing 2 mL of PBS each.

Cells were seeded as reported previously, at a concentration of 0.2×10^6 cells/mL on each microwell in cell culture media droplets of 200 μL, which were allowed to incubate at room temperature for 5 minutes. The remaining 1800 μL of cell culture media was added, for a final volume of 2 mL per well. The plates were placed in the cell culture incubator and 1 mL of warmed cell culture media was exchanged every 2 days for a week to allow for spheroid aggregation. Spheroid formation was monitored using an Olympus microscope (Olympus, Tokyo, Japan).

C. IC-50 DETERMINATION AND DRUG ADMINISTRATION

An MTT assay was conducted to calculate the IC-50 of AAAPT drug, AMP-001, from the resulting cell viability. LN229 cells were seeded in 96-well flat-bottom plates at the density of 5×10^5 per well and allowed to attach overnight. A 2:1 dilution of AMP-001, beginning at 100 μM, was formulated to treat cells in 3 technical replicates per concentration. Treatments were applied and the cells were incubated again for 24 hours. Then, 10 μl (3–45-dimethylthiazol-2-yl)-25-diphenyltetrazolium bromide (Roche) were added to each well and the plate was incubated in the cell culture incubator for 3 hours. To dissolve the crystals, 100 μl of solubilization buffer was added. Absorbance was read at 550 nm in an Epoch plate reader (BioTek, Winooski, VT), normalized to a reading of the blank well, filled with cell culture media only. The concentration at which the cells demonstrated 50% cell viability of the untreated well was determined to be the IC-50 (52 μM) for AMP-001.

The IC-50 was then used to treat the microwells which had grown for a week and developed into spheroids. AMP-001 was weighed and dissolved in MilliQ water, freshly for each experiment. The drug was then diluted in 2 mL of cell culture media to the appropriate concentration and gently administered to the proper wells after the initial cell culture media was

removed. The spheroids were incubated and monitored using an Olympus microscope (Olympus, Tokyo, Japan). AMP-001 was compared to previously determined concentration (300 μM) of the traditional chemotherapy treatment.

D. CELL VIABILITY QUANTIFICATION

Trypan blue cell viability assay was conducted by first collecting the cells after washing with PBS and incubation with trypsin. Cells were stained with 0.4% trypan blue solution, counted using a hemocytometer, and cell viability was calculated by normalization to the control group.

E. QUANTITATIVE REVERSE TRANSCRIPTION PCR

Total RNA from LN229 cells, which had been cultured into spheroids in microwells, were extracted and purified using the RNeasy Kit (Qiagen, Germantown, MD, USA). The RNA concentration was quantified using a Nanodrop (Thermo Fisher Scientific, Houston, TX), where the optical density (OD) was measured at 260 and 280 nm. Reverse transcription was performed to produce cDNA using the High-Capacity cDNA Reverse Transcription Kit with RNase Inhibitor (Thermo Fisher Scientific, Houston, TX). Using the StepOnePlus Real-Time PCR System (Thermo Fisher Scientific, Houston, TX), qPCR was conducted in 20 μL reactions. Primer sequences for the pre-formulated BAX, BCL-2, and GAPDH Taqman Gene Expression Assays (Thermo Fisher Scientific, Houston, TX) utilized are unknown, but were selected to span exons, to prevent gDNA replication. Each reaction mixture contained 14 ng of cDNA, 10 μL of Master Mix and 1 μL of the specific Taqman Gene Expression Assay. The plates were run for 2 min at 50 °C, 20 seconds at 95 °C, and both 1 second at 95 °C and 20 seconds at 60 °C for 40 cycles.

F. WESTERN BLOT

After washing with cold PBS, protein was extracted from the spheroids using cold RIPA Lysis Buffer, including freshly added protease inhibitor cocktail and phosphatase inhibitor cocktail 3 (Sigma-Aldrich), and a cell scraper. Cell lysates were incubated on ice for 5 minutes, then centrifuged at 4 °C, 16000 rpm for 10 min. The supernatants were collected, and a Micro BCA Kit (Thermo Fisher Scientific, Houston, TX) was used to determine the protein concentration of each biological sample. A cell lysate mass of 50 μg from each sample was subjected to 12% SDS-PAGE gels in 1x Running Buffer and transferred onto a methanol activated, PVDF membrane (Thermo Fisher Scientific, Houston, TX, USA) in 1x Transfer Buffer. Membranes were blocked with 5% milk (in 1 $\times$ TBST) for 1 hour, then underwent primary antibody incubation overnight at 4 °C. Following three, 5-minute washes of TBST, membranes were incubated with secondary antibody in appropriate buffer for 1 hour. Separated protein bands were visualized using ECL Western blot detection solution (Amersham Pharmacia Biotech) and imaged. BAX, BCL-2, GAPDH, and β-Actin (Cell Signaling Technology, Danvers, MA, USA) antibodies were used at a concentration of 1:500. Goat anti-Mouse IgG (H+L) Secondary Antibody (HRP) (Cell Signaling Technology, Danvers, MA, USA) was used at 1:2000 concentration. The expression data were normalized to GAPDH and β-actin.

G. STABILITY ASSAY

AMP-001 (10 μL of 100 μM DMSO stock solution) was added to 490 μL of the selected matrix. Final concentration of test compound in the assay is 2 μM and final organic (DMSO) content in the assay is 2%. Immediately after adding AMP-001, 50 uL aliquot is taken, and was mixed with 200 uL of acetonitrile containing Carbamazepine as internal standard (10 ug/mL). Remaining 450 uL reaction is incubated at 37 °C, and at various time-points (0, 1, 2, 4, 6, 24 hours) aliquots were withdrawn and the reaction was stopped with acetonitrile as an internal standard. Precipitated protein was removed by a brief centrifugation and the supernatant was analyzed by LC-MS/MS. Compound stability was calculated and reported as % PCR (% parent compound remaining relative to untreated control, (% PCR = ("n^{th}" minute sample area ratio/zero-minute sample area ration) x 100 (PCR = Percent parent compound remaining; n = specific time-point), Area Ratio = (Analyte Area in LC-MS/MS)/(internal standard Area in LC-MS/MS).

H. STATISTICAL ANALYSIS

All reported results were from three independent experiments performed in triplicate. The unpaired two-tailed Student's t-test was employed for statistical comparisons between groups, where a p value < 0.05 indicated a statistically significant difference between values. The data were displayed as the average $\pm$ standard deviation.

III. RESULTS

A. CELL VIABILITY AND DRUG ADMINISTRATION

As a proof of concept in verifying the effect of AMP-001 on GBM cell line, LN229, an IC-50 assay was conducted. LN229 cells were plated at a concentration of 5×10^5 cells/mL and treated with AMP-001 in dilution. MTT indicated that the IC-50 for AMP-001 on LN229 GBM cells was 52 μM (Fig. 1). This is within the range of other approved drugs by the FDA for cancer chemotherapy treatment [31]. AMP-001 was used alone or in combination with TMZ at a concentration of 300 μM [18]. Control microwells went untreated and were allowed to grow unhindered by any manipulation.

To understand the proposed drug's effect on the 3D spheroids, cell viability assay was performed after the drugs were introduced. As shown in (Fig. 2(a)), the drug treatments resulted in a decrease in spheroid diameter and therefore also decreasing the viability of cells, with AMP-001 most strongly decreasing cell viability ($p < 0.01$). The cell viability of the spheroids after 7 days of treatment were normalized to the viability of the control group and determined to be 19.94 $\pm$ 2.98% after AMP-001, and 45.45 $\pm$ 1.54% after TMZ treatment. The data demonstrated that the novel AMP-001

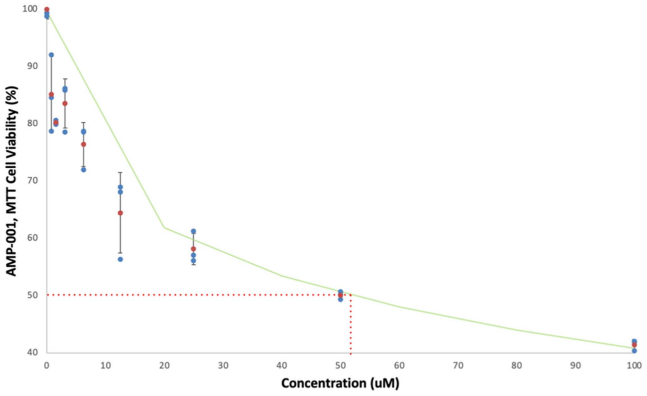

FIGURE 1. IC-50 of AMP-001 in LN229 cell line, via MTT colorimetric assay. The concentration related to the 50% survival of total LN229 cells as determined to be 52 μM. Student's T-test conducted, where data represent the mean ± SD of three biological replicates, $p < 0.05$.

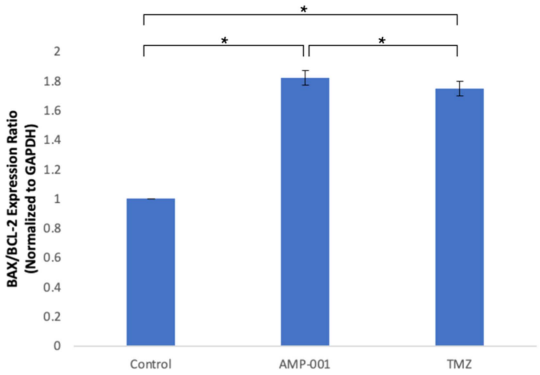

FIGURE 3. Drug treatment results in RT-qPCR BAX/BCL-2 (ratio >1). Real time qPCR fold-change results, in BAX to BCL-2 ratio, normalized to the control (=1). Ratios >1 indicate an increase in ratio from the control, upregulation of cell death pathways, and downregulation in cell survival pathways. Data represents the mean ± SD of three biological replicates. A student's T-test was conducted between each biological group. ∗ indicates $p < 0.05$.

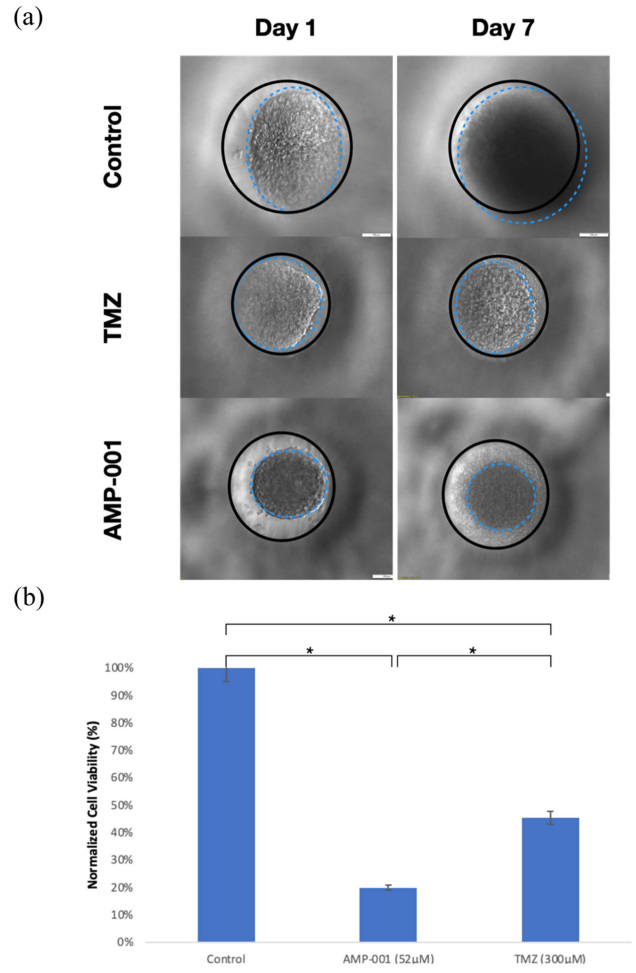

FIGURE 2. Representative images of treated GBM spheroids in PEGDA microwells. (a) Representative images of LN229 cells in the PEGDA microwells (400 μm) after 7 days of drug administrations: Control, TMZ, and AMP-001. Effects of the drug treatment were visualized by the disaggregation of the dead cells on day 7 of treatment. X20 objective. Scale bars, 100 μm. (b) Normalized viability of LN229 cells after treatment using trypan blue staining. Data represents the mean ± SD of three biological replicates. Student's T-test was conducted between biological groups. ∗ indicates $p < 0.01$.

treatment was more effective than using chemotherapy gold standard, TMZ treatment, at a lower dose.

B. GENE EXPRESSION STUDIES

To understand the changes in the key apoptotic markers BAX and BCL-2 after drug treatment, gene expression analysis was completed.

LN229 cells were seeded in the aforementioned microwells at 0.2×10^6 cells/mL, cultured into spheroids for 7 days and treated. Using RT-qPCR, gene expression analysis was assessed. An increase in BAX expression and a decrease in BCL-2 expression was observed in the treatment groups in comparison to the control. This subsequently lead to a BAX/BCL-2 ratio of greater than 1 for all treatment groups (Fig. 3), with the AMP-001 group showing the highest ratio at 1.82 ± 3.4%, in comparison to TMZ at 1.75 ± 4.1%, when normalized to expression of the control group (Fig. 2).

C. WESTERN BLOT

Confirmation of qPCR results, studying sensitization-indicative genes, was conducted with western blot. The expression of BAX (cell death indicator), in comparison to the control group and normalized by the intensity of GAPDH, increased in AMP-001 by 35%. BCL-2 (cell survival indicator) expression minorly increased, in the combination treatment group, by 2%. A p value of less than or equal to 0.05 was calculated for all groups, demonstrating significance in the difference of expression. When converted into a ratio of BAX/BCL-2 (Fig. 4(a) and (b)), the overall increase from the control group was 32% for AMP-001, reflecting a ratio of 1.32. NF-κB (p65) expression decreased in the treated cells by 45%, while CD95 increased by 21% from the control group.

For further mapping of the affected protein expression pathways, NF-κB (p65) and CD95 were investigated post AMP-001 treatment, versus a control (Fig. 4(c), (d), and (e)). NF-κB

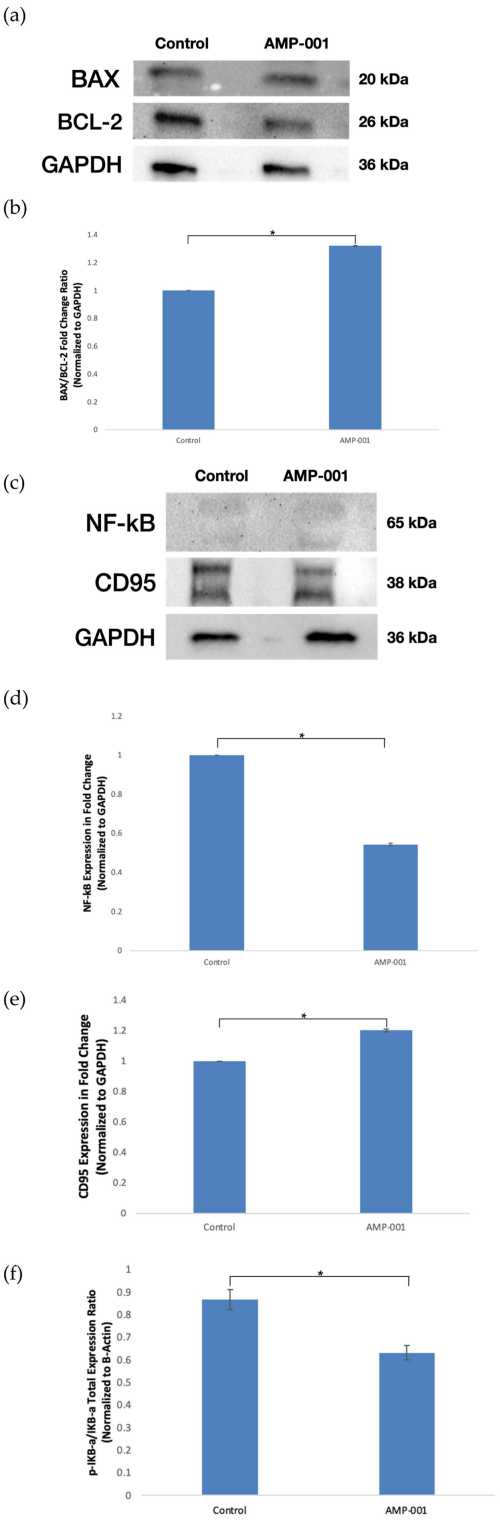

FIGURE 4. Effect of AMP-001 and TMZ on protein expression. BAX and BCL-2 activity (normalized by GAPDH) in LN229 spheroids treated with or without AMP-001, collected from the microwells and subjected to western blot as visualized by (a) raw blot and (b) a graph of the BAX/BCL-2 ratio. (c) NF-κB (p65) and CD95 (normalized by GAPDH), as well as P-IKB-a and IKB-a (normalized by B-actin) representative immunoblots. The (d) (e) fold change ratios for NF-κB (p65) and CD95 and (f) phosphorylated versus total IKB-a expression ratios. Student's T-test conducted, where data represent the mean $\pm$ SD of three biological replicates. $*$ indicates $p < 0.05$.

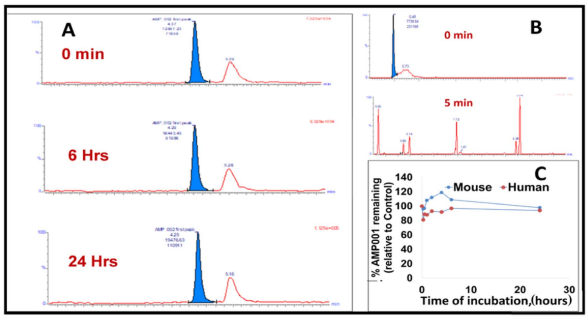

FIGURE 5. Stability of AMP-001 in human and mouse plasma using LC-MS. (a) The peak area under AMP-001 did not change significantly up to 24 hours in human plasma, (b) stability of control procain in human plasma which gets degrades in 5 mins, $p < 0.004$, $n = 4$.

(p65), representative of cell survival, demonstrated a significant 45% decrease in AMP-001 groups in comparison to the control. CD95, indicative of cell apoptosis, showed a significant 21% increase in AMP-001 groups versus the control.

Finally, to verify NF-κB inactivation in AMP-001 treated groups, the phosphorylation of IKB-a was studied. AMP-001 treated spheroids demonstrated a 24% decrease in expression of p-IKB-a, divided by total IKB-a expression, in comparison to control groups (Fig. 4(c) and (f)).

D. STABILITY OF AMPS

Stability of drugs in either serum or in blood plays an important part of the drug design so that there is a sufficient concentration of the drug that circulates in the blood stream for long time enough to reach the tumor. Stability assessment also reveals the presence of potential metabolites and their clearance.

We have investigated stability of AMP-001 after incubation with both human and mouse plasma for greater than 24 hours. Procaine as a reference compound was used and the stability was quantified using LC-MS/MS method, specifically developed and calibrated for stability assay. Fig. 5(a) shows time-dependent stability of AMP-001 over 24hours which is graphically depicted in Fig. 5(b). On the contrary, the control Procaine degraded very fast in few minutes (Fig. 5(c)).

IV. DISCUSSION

GBM is highly treatment resistant due to activating pathways which promote cell survival and deactivating those that promote cell death. TMZ, its gold standard chemotherapy treatment, is non-specific, leading to damage of important surrounding tissues. Both factor into a high recurrence probability and overall low survival rates. Care must be improved to increase the quality of life for GBM patients. Screening of drugs through the microwell platform allows for an in vitro, fast comparison of outcomes and analysis of the mechanisms behind triggering apoptosis in treatment resistant cells. AMP-001, which has been shown to have the possibility to treat other cancers as in prostate, lung, and triple negative breast cancer (TNBC) [20], [21], was proposed to have a potential

to treat GBM through similar mechanisms. In the case of discovering a new drug like AMP-001, utilizing the microwell assay allows for efficient screening to verify its capabilities as a targeted tumor sensitizing agent. This is especially true, in that the use of spheroids which have been shown to be efficient to generate and act as an accurate representation of tumors in vivo. 3D culturing recapitulates characteristics of in vivo tumors such as cell–cell and cell–ECM interactions, nutrient and oxygen gradients, and layers of cell populations, gene expression and activation of cell signaling pathways [32]. Accuracy on the lab bench will help to translate the results more precisely to patient treatment.

By understanding the desensitization mechanisms in tumors which inactivate or downregulate specific cell death pathways and reactivate cell survival pathways, drugs can also be designed to induce sensitization more specifically in cells which show low response to therapy. Specificity means decreased cardiotoxicity, which is beneficial since systemic desensitization can induce poor outcomes such as neurodegeneration, myelosuppression, and more, without much positive contribution to cancer survival [33], [34], [35]. This is how AAAPT, AMP-001 has been shown to serve in potential chemotherapy regimens. AMP-001 spares normal cells from off-target effects, by releasing the drug near tumor sites and only activating upon the cleavage of its valine-citrulline link. This linkage is only cleavable by tumor-specific biomolecule Cathepsin B, which is highly upregulated by malignant tumors in comparison to normal tissues and becomes attached to the tumor surface [36], [37], [38], [39]. Furthermore, due to its pegylation AMP-001 is water soluble, enhancing it's by keeping it intact in blood circulation until reaching pertinent tumor cells [20], [21]. The BAX/BCL-2 ratio is a well-known identifier of such capabilities and can act as a proof-of-concept biomarker for the effectiveness of new chemotherapy proposals. Observing an increase in the ratio to a value above 1, signifies a higher value of BAX (apoptosis pathways triggered) expression than BCL-2 (cell survival pathways triggered) expression, meaning that the drug is able re-sensitize the cells [24], [25]. In our previous studies, TMZ has shown to have this effect, especially in synergy with NF-κB inhibitor, BAY-11-7082 [18]. For this reason, the BAX and BCL-2 biomarkers were chosen to observe in both RT-qPCR and western blot. NF-κB (p65) and p-IKB-a, as well as CD95 were also chosen as biomarkers in that they too play a role in resistance to cell death and cell death signaling, respectively. Damage to DNA initiates NF-κB (a complex of heterodimers, RelA/p65 and p50) to orchestrate DNA repair by acting as a transcription factor, ultimately aiding cell survival [40]. The presence of IKB inhibits NF-κB expression, but the phosphorylation of IKB-a is known to degrade IKB [41]. Therefore, p-IKB-a expression results in cell desensitization, although it must be viewed with respect to the overall IKB-a protein expression to demonstrate that the change in phosphorylated protein is not due to variation in total protein across treatment groups. CD95 is triggered by CD95 ligand, setting off caspase-3 and 8 to promote cell death [42].

Before gene and protein expression studies, the IC-50 was determined in order to utilize the lowest effect concentration possible in our study. Although AMP-001 is meant to be specific, reducing the drug concentration should result in further reducing the potential of off target effects. An MTT assay following the treatment of GBM cells with AMP-001, determined that a 52 μM concentration would be enough to cause apoptosis in half of the cells available. This is in comparison to the 300 μM concentration, previously determined to be necessitated by the TMZ treatment. Similarly in previous AAAPT studies, 50 μM was determined as the IC-50 in other cancers [10]. Further testing may be done to optimize the concentration of AMP-001 for GBM alone or in synergy with another drug. Trypan blue staining of GBM spheroids treated with AMP-001 or TMZ revealed that there was a steeper decrease in the number of cells which survived in the presence of both AMP-001. When normalized to the control for comparison, only about 20% of the AMP-001 treated cells survived at the treatment 7-day mark. It can also be observed via imaging, that the spheroids became less tightly bound and dispersed at a faster rate in the AMP-001 treated biological group than in the other groups. This is similar to the results from our previous studies, indicating that the cell death following TMZ can be improved. The significance of the novel drug AMP-001 demonstrating higher cytotoxicity in GBM cells is that it may be able to replace TMZ, at a lower concentration, and systemic toxicity can be avoided.

Cancer cells which demonstrate a sensitivity to drug treatment are believed to have triggered a cell pathway altering the expression of BAX and BCL-2. The two genes have been shown to previously correlate inversely: BAX as an indicator of sensitivity to apoptosis and BCL-2 as an indicator of resistance. Previously, we have demonstrated using microwells in our lab that TMZ and BAY-11-7082 in combination trigger such a response in GBM, leading to an increase in cell death. Ratio values greater than 1 relay the increase in BAX expression, or cell death pathway down regulation, and a relatively lower BCL-2 expression, indicating cell survival pathway upregulation. Using RT-qPCR, AMP-001 was found to cause an increase in the BAX/BCL-2 ratio, significantly, from the control.

Under western blot, the AMP-001 treated sample group reflected an increase in BAX expression, and slight increase in BCL-2 expression, resulting in an overall increased BAX/BCL-2 ratio, which matches our RT-qPCR result. From prior experiments in our lab, it has been found that TMZ both induces cell death and increases the BAX/BCL-2 ratio, just as AMP-001 treatment has shown in this study. Yet, the concentration of the AMP-001 treatment is more targeted and smaller in dose. Further investigation of the protein expression pathways via western botting included NF-κB (p65), p-IKB-a, and CD95. Phosphorylated IKB-a is initially upregulated in cancers to degrade IKB-a and subsequently activate the NF-κB pathway. Upregulation of NF-κB is common in GBM to evade treatments such as those that methylate DNA [43]. Cancer cells tend to obtain advantages to survive during

tumor growth by decreasing their sensitivity to CD95-induced apoptosis, often by downregulating CD95 expression [44]. The AMP-001 treated group indicated cell sensitization via the down regulation of NF-κB (p65), which was verified by the phosphorylation of IKB-a (relative to total IKB-a) expression. Cell sensitization was also indicated by an upregulation of CD95 expression. RT-qPCR and western blot data, paired with the cell viability data, demonstrates a correlation between AMP-001 triggering the investigated pathways and cell death, leading to the conclusion that the cells were likely sensitized via the AMP-001 treatment.

The translation of preclinical to potential clinically viable drug mainly depends on the stability of the drug in either serum or blood in situ and further in vivo. Our preliminary data on AMP-001 subjected to time dependent quantification of the remaining AMP-001 intact for 24 hours in human serum clearly indicates that AMP-001 did not undergo any significant degradation in sera. On the contrary, the control Procain degraded fast to show that stability assessment was carried out in control conditions.

V. CONCLUSION

Here, we have developed a rapid proof of concept study, using our previously developed microwells, for the novel drug, AMP-001. AMP-001has shown promise as a re-sensitizing drug for lung and breast cancers. In this study, we confirmed that AMP-001 could be used as a promising therapeutic approach for GBM, compared to chemotherapy gold-standard, Temozolomide, at only about 17% of the dosage. Thereby, off-target effects may be reduced at greater effectiveness and patient survival rate may also improve. Future studies should aim to increase knowledge of the pathways triggered by AMP-001, such as recent findings that support the activation of NF-κB by eEF2K in most cancers, therefore rendering it a possible therapeutic target [45], [46], [47]. Studies may also aim to optimize the treatment for delivery to the blood-brain barrier, and to dynamically co-culture cells with other important tissues to further investigate the specificity of mechanisms which serve to decease off-target effects [48], [49], [50], [51].

CONTRIBUTIONS

Megan Mendieta, Naze G. Avci, Yasemin M. Akay, and Metin Akay designed the experiment. Megan Mendieta conducted the experiments. Megan Mendieta, Naze G. Avci, Yasemin M. Akay, and Metin Akay analyzed and interpreted the data. Megan Mendieta, Naze G. Avci, Yasemin M. Akay, Metin Akay and Raghu Pandurangi wrote and reviewed the manuscript.

ACKNOWLEDGMENT

Authors would like to thank Dr. Tina Kazemi for advising on the study. Funding organizations did not play any roles in designing experiments, data collection, analysis, or any decision to publish the data.

REFERENCES

[1] M. Koshy et al., "Improved survival time trends for glioblastoma using the SEER 17 population-based registries," *J. Neuro-Oncol.*, vol. 107, no. 2, pp. 207–212, 2012, doi: 10.1007/s11060-011-0738-7.

[2] F. Hanif, K. Muzaffar, K. Perveen, S. M. Malhi, and S. U. Simjee, "Glioblastoma multiforme: A review of its epidemiology and pathogenesis through clinical presentation and treatment," *Asian Pacific J. Cancer Prevention*, vol. 18, no. 1, pp. 3–9, 2017, doi: 10.22034/APJCP.2017.18.1.3.

[3] Q. T. Ostrom et al., "CBTRUS statistical report: Primary brain and other central nervous system tumors diagnosed in the United States in 2012-2016," *Neuro-Oncol.*, vol. 21, pp. v1–v100, 2019, doi: 10.1093/neuonc/noz150.

[4] S. S. Kitambi et al., "Vulnerability of glioblastoma cells to catastrophic vacuolization and death induced by a small molecule," *Cell*, vol. 157, no. 2, pp. 313–328, 2014, doi: 10.1016/j.cell.2014.02.021.

[5] Q. T. Ostrom et al., "The epidemiology of glioma in adults: A 'state of the science' review," *Neuro-Oncol.*, vol. 16, no. 7, pp. 896–913, 2014, doi: 10.1093/neuonc/nou087.

[6] M. Hegi et al., "MGMT gene silencing and benefit from temozolomide in glioblastoma," *New England J. Med.*, vol. 352, no. 10, pp. 997–1003, 2005, doi: 10.1056/NEJMoa043331.

[7] C. H. Fan, W. L. Liu, H. Cao, C. Wen, L. Chen, and G. Jiang, "O6-methylguanine DNA methyltransferase as a promising target for the treatment of temozolomide-resistant gliomas," *Cell Death Dis.*, vol. 4, no. 10, 2013, Art. no. e876, doi: 10.1038/cddis.2013.388.

[8] F. Pistollato et al., "Intratumoral hypoxic gradient drives stem cells distribution and MGMT expression in glioblastoma," *Stem Cells*, vol. 28, no. 5, pp. 851–862, 2010, doi: 10.1002/stem.415.

[9] C. Friesen, S. Fulda, and K. M. Debatin, "Deficient activation of the CD95 (APO-1/Fas) system in drug-resistant cells," *Leukemia*, vol. 11, no. 12, pp. 1833–1841, 1997, doi: 10.1038/sj.leu.2400827.

[10] P. H. Krammer, "The tumor strikes back. New data on expression of the CD95 (APO-1/Fas) receptor/ligand system may cause paradigm changes in our view on drug treatment and tumor immunology," *Cell Death Differentiation*, vol. 4, no. 4, pp. 362–364, 1997, doi: 10.1038/sj.cdd.4400252.

[11] U. Ramp et al., "Deficient activation of CD95 (APO-1/Fas)-mediated apoptosis: A potential factor of multidrug resistance in human renal cell carcinoma," *Brit. J. Cancer*, vol. 82, no. 11, pp. 1851–1859, 2000, doi: 10.1054/bjoc.2000.1155.

[12] Y. Fan et al., "Engineering a high-throughput 3-D in vitro glioblastoma model," *IEEE J. Transl. Eng. Health Med.*, vol. 3, 2015, Art. no. 4300108, doi: 10.1109/JTEHM.2015.2410277.

[13] F. Pampaloni, E. G. Reynaud, and E. H. K. Stelzer, "The third dimension bridges the gap between cell culture and live tissue," *Nature Rev. Mol. Cell Biol.*, vol. 8, no. 10, pp. 839–845, 2007, doi: 10.1038/nrm2236.

[14] N. Zahir and V. M. Weaver, "Death in the third dimension: Apoptosis regulation and tissue architecture," *Curr. Opin. Genet. Develop.*, vol. 14, no. 1, pp. 71–80, 2004, doi: 10.1016/j.gde.2003.12.005.

[15] J. B. Kim, "Three-dimensional tissue culture models in cancer biology," *Seminars Cancer Biol.*, vol. 15, no. 5, pp. 365–377, 2005, doi: 10.1016/j.semcancer.2005.05.002.

[16] O. S. Agboola, X. Hu, Z. Shan, and M. Majumder, "Brain organoid: A 3D technology for investigating cellular composition and interactions in human neurological development and disease models in vitro," *Stem Cell Res. Ther.*, vol. 12, no. 1, 2021, Art. no. 430, doi: 10.1186/s13287-021-02369-8.

[17] M. J. Rybin, M. E. Ivan, N. G. Ayad, and Z. Zeier, "Organoid models of glioblastoma and their role in drug discovery," *Front. Cellular Neurosci.*, vol. 15, 2021, Art. no. 605255, doi: 10.3389/fncel.2021.605255.

[18] N. G. Avci et al., "NF-κB inhibitor with temozolomide results in significant apoptosis in glioblastoma via the NF-κB(p65) and actin cytoskeleton regulatory pathways," *Sci. Rep.*, vol. 10, no. 1, 2020, Art. no. 13352, doi: 10.1038/s41598-020-70392-5.

[19] S. E. Pustchi, N. G. Avci, Y. M. Akay, and M. Akay, "Astrocytes decreased the sensitivity of glioblastoma cells to temozolomide and bay 11-7082," *Int. J. Mol. Sci.*, vol. 21, no. 19, 2020, Art. no. 7154, doi: 10.3390/ijms21197154.

[20] R. Pandurangi, "Compositions and methods for sensitizing low-responsive tumors to cancer therapy," Patent Cooperation Treaty, PCT/US16/68554, 2016.

[21] R. S. Pandurangi, O. Cseh, H. A. Luchman, C. X. Ma, S. N. Senadheera, and M. L. Forrest, "CD95 structure, aggregation and cell signaling," *Amer. Chem. Soc. Pharmacol. Transl. Sci.*, vol. 6, no. 3, pp. 372–386, 2023, doi: 10.1021/acsptsci.2c00091.
[22] N. Aggarwal and B. F. Sloane, "Cathepsin B: Multiple roles in cancer," *Proteomic. Clin. Appl.*, vol. 8, no. 5/6, pp. 427–437, 2014, doi: 10.1002/prca.201300105.
[23] K. Ma, X. Chen, W. Liu, and Y. Shang, "CTSB is a negative prognostic biomarker and therapeutic target associated with immune cells infiltration and immunosuppression in gliomas," *Sci. Rep.*, vol. 12, no. 1, 2022, Art. no. 4295, doi: 10.1038/s41598-022-08346-2.
[24] F. E. McDonald et al., "The prognostic influence of Bcl-2 in malignant glioma," *Brit. J. Cancer*, vol. 86, no. 12, pp. 1899–1904, 2002, doi: 10.1038/sj.bjc.6600217.
[25] Z. N. Oltvai, C. L. Milliman, and S. J. Korsmeyer, "Bcl-2 heterodimerizes in vivo with a conserved homolog, Bax, that accelerates programmed cell death," *Cell*, vol. 74, no. 4, pp. 609–619, 1993, doi: 10.1016/0092-8674(93)90509-O.
[26] D. Verzella, A. Pescatore, D. Capece, and F. D. Vecchio, "Life, death, and autophagy in cancer: NF-κB turns up everywhere," *Cell Death Dis.*, vol. 11, no. 3, p. 210, 2020, doi: 10.1038/s41419-020-2399-y.
[27] J. L. Luo, H. Kamata, and M. Karin, "IKK/NF-κB signaling: Balancing life and death–a new approach to cancer therapy," *J. Clin. Investigation*, vol. 115, no. 10, pp. 2625–2632, 2005, doi: 10.1172/JCI26322.
[28] M. Djavaheri-Mergny et al., "NF-κB activation represses tumor necrosis factor-alpha-induced autophagy," *J. Biol. Chem.*, vol. 281, no. 41, pp. 30373–30382, 2006, doi: 10.1074/jbc.M602097200.
[29] M. E. Peter, A. Hadji, A. Murmann, and S. Brockway, "The role of CD95 and CD95 ligand in cancer," *Cell Death Differentiation*, vol. 22, no. 4, pp. 549–559, 2015, doi: 10.1038/cdd.2015.3.
[30] A. Haluck-Kangas and M. E. Peter, "CD95/Fas ligand induced toxicity," *Biochem. Soc. Trans.*, vol. 51, no. 1, pp. 21–29, 2020, doi: 10.1042/BST20211187.
[31] M. T. C. Poon, M. Bruce, J. E. Simpson, and K. C. H. Fearon, "Temozolomide sensitivity of malignant glioma cell lines – A systematic review assessing consistencies between in vitro studies," *BioMed Central Cancer*, vol. 21, no. 1, 2021, Art. no. 1240, doi: 10.1186/s12885-021-08972-5.
[32] B. Pinto, A. C. Henriques, P. M. A. Silva, and A. R. Neves, "Nanoparticles for targeted brain drug delivery: What do we know?," *Int. J. Mol. Sci.*, vol. 22, no. 21, 2020, Art. no. 11654, doi: 10.3390/ijms222111654.
[33] V. Schirrmacher, "From chemotherapy to biological therapy: A review of novel concepts to reduce the side effects of systemic cancer treatment," *Int. J. Oncol.*, vol. 54, no. 2, pp. 407–419, 2019.
[34] G. Morgan, R. Ward, and M. Barton, "The contribution of cytotoxic chemotherapy to 5-year survival in adult malignancies," *Clin. Oncol.*, vol. 16, no. 8, pp. 549–560, 2004, doi: 10.1016/j.clon.2004.06.007.
[35] S. Niraula, E. Amir, F. Vera-Badillo, B. Seruga, A. Ocana, and I. F. Tannock, "Risk of incremental toxicities and associated costs of new anticancer drugs: A meta-analysis," *J. Clin. Oncol.*, vol. 32, no. 32, pp. 3634–3642, 2014, doi: 10.1200/JCO.2014.55.8437.
[36] J. Mai, D. M. Waisman, and B. F. Sloane, "Cell surface complex of cathepsin B/annexin II tetramer in malignant progression," *Biochimica Biophysica Acta*, vol. 1477, no. 1/2, pp. 215–230, 2000, doi: 10.1016/s0167-4838(99)00274-5.
[37] J. Mai, R. L. Finley Jr., D. M. Waisman, and B. F. Sloane, "Human procathepsin B interacts with the annexin II tetramer on the surface of tumor cells," *J. Biol. Chem.*, vol. 275, no. 17, pp. 12806–12812, 2000, doi: 10.1074/jbc.275.17.12806.
[38] O. Vasiljeva, T. Reinheckel, C. Peters, D. Turk, V. Turk, and B. Turk, "Emerging roles of cysteine cathepsins in disease and their potential as drug targets," *Curr. Pharmaceut. Des.*, vol. 13, pp. 387–403, 2007, doi: 10.2174/138161207780162962.
[39] A. Purr, "Cathepsin in rats with transplantable cancer," *Biochem. J.*, vol. 28, pp. 1907–1910, 1934.
[40] S. Janssens and J. Tschopp, "Signals from within: The DNA-damage-induced NF-κB response," *Cell Death Differentiation*, vol. 13, no. 5, pp. 773–784, 2006, doi: 10.1038/sj.cdd.4401843.
[41] F. Christian, E. L. Smith, and R. J. Carmody, "The regulation of NF-κB subunits by phosphorylation," *Cells*, vol. 5, no. 1, 2016, Art. no. 12, doi: 10.3390/cells5010012.
[42] N. Levoin, M. Jean, and P. Legembre, "CD95 structure, aggregation and cell signaling," *Front. Cell Devlop. Biol.*, vol. 8, 2020, Art. no. 314, doi: 10.3389/fcell.2020.00314.
[43] V. T. Puliyappadamba, K. J. Hatanpaa, S. Chakraborty, and A. A. Habib, "The role of NF-κB in the pathogenesis of glioma," *Mol. Cellular Oncol.*, vol. 1, no. 3, 2014, Art. no. e963478, doi: 10.4161/23723548.2014.963478.
[44] E. Ametller, S. García-Recio, D. Costamagna, V. Almendro, and J. Arribas, "Tumor promoting effects of CD95 signaling in chemoresistant cells," *Mol. Cancer*, vol. 9, 2010, Art. no. 161, doi: 10.1186/1476-4598-9-161.
[45] L. Temme and C. R. M. Asquith, "eEF2K: An atypical kinase target for cancer," *Nature Rev. Drug Discov.*, vol. 20, no. 8, 2020, Art. no. 577, doi: 10.1038/d41573-021-00124-5.
[46] M. A. Erdogan, A. Ashour, E. Yuca, K. Gorgulu, and B. Ozpolat, "Targeting eukaryotic elongation factor-2 kinase suppresses the growth and peritoneal metastasis of ovarian cancer," *Cellular Signalling*, vol. 81, 2021, Art. no. 109938, doi: 10.1016/j.cellsig.2021.109938.
[47] D. Karakas and B. Ozpolat, "Eukaryotic elongation factor-2 kinase (eEF2K) signaling in tumor and microenvironment as a novel molecular target," *J. Mol. Med.*, vol. 98, no. 6, pp. 775–787, 2020, doi: 10.1007/s00109-020-01917-8.
[48] N. G. Avci, Y. Fan, A. Dragomir, Y. M. Akay, and M. Akay, "Investigating the influence of HUVECs in the formation of glioblastoma spheroids in high-throughput three-dimensional microwells," *IEEE Trans. Nanobiosci.*, vol. 14, no. 7, pp. 790–796, Oct. 2015, doi: 10.1109/TNB.2015.2477818.
[49] D. Marchetti, J. Li, and R. Shen, "Astrocytes contribute to the brain-metastatic specificity of melanoma cells by producing heparanase," *Cancer Res.*, vol. 60, no. 17, pp. 4767–4770, 2000.
[50] R. G. R. Pinheiro, A. J. Coutinho, M. Pinheiro, and A. R. Neves, "Nanoparticles for targeted brain drug delivery: What do we know?," *Int. J. Mol. Sci.*, vol. 22, no. 21, 2021, Art. no. 11654, doi: 10.3390/ijms222111654.
[51] G. Kara, B. Arun, G. A. Calin, and B. Ozpolat, "miRacle of microRNA-driven cancer nanotherapeutics," *Cancers*, vol. 14, no. 15, 2022, Art. no. 3818, doi: 10.3390/cancers14153818.